

Proceedings of

12th Structural Engineering Convention - An International Event (SEC 2022)



Available at https://asps-journals.com/index.php/acp

Confinement detailing of concrete encased steel concrete composite columns

Sunny Mishra^{1*}, S.R. Satish Kumar²

¹Department of Civil Engineering, Research scholar, Indian Institute of Technology, Madras, 600036, India ²Department of Civil Engineering, Professor, Indian Institute of Technology, Madras, 600036, India

Paper ID - 010511

Abstract

Steel concrete composite construction is now gaining popularity in our country. Concrete-encased steel columns have several advantages, but like RC columns, there is a need to ensure adequate concrete confinement so that it has sufficient ductility under seismic loads. This study investigates the confinement of the concrete based on the detailing of the transverse reinforcement. The ductilities of a typical encased section that satisfies the minimum reinforcement criteria and a highly confined sectionwith special detailing are compared. A nonlinear 3D finite element model is developed in ABAQUS for this purpose. The confined stress-strain curve for M30 grade of concrete is carefully incorporated in the special confined section. The interaction between structural steel and concrete is modelled with an 'embedded region' interaction tool available in the ABAQUS library. Based on the eigen mode of the section, theinitial geometric imperfection wasgiven. The significant increment in displacement ductility factor, plastic hinge rotation and drift ratio are observed for a special confined encased column. A parametric study has been carried out by varying the parameters; the axial load ratio, steel contribution ratio, steel width to depth ratio and transverse reinforcement spacing. It was observed thatstructural section aspect ratio (steel width to depth) and transverse reinforcement spacing significantly affect the ductility of the section. The plastic hinge rotation and drift ratios were also calculated for different sections.

Keywords: Encased composite columns; confinement of concrete; Ductility; Finite element analysis; Axial load ratio.

1. Introduction

In the developing era of high-rise buildings, most buildings in India are either non-engineered or poorly designed RC structures. The steel structure is also being used a lot in the last few decades, but the central problems of steel are corrosion and fire resistance. If we use a composite of concrete and steel, a new, better structure can be made, which can eliminate the shortcomings of steel and concrete. Although the initial cost will be higher than an RC frame, the fast rate of construction and durability make it economical in the long run, and sosteel concrete composite constructions are becoming very popular in our country. Therefore, it is necessary to know the behaviour of composite sections during an earthquake. This study focuses on the ductility of concrete-encased steel concrete composite columns. The concrete surrounding the steel in encased sectionincreases strength and stiffness and protects from fire damage. In this way, the composite column can become an ideal solution for seismic regions. The structural steel can take most of the dead load, so structures will remain standingeven if concrete spalling and longitudinal bar buckling occurs during a severe earthquake. However, the detailing of longitudinal and transverse reinforcement is a

primary concern for designers. Researchers have investigated the encased composite column subjected to axial load and major or minor axis bending[1,2]. The composite column has increased load-carrying capacity, deformation capacity, energy dissipation, and the surrounding concrete prevents the local buckling of flanges and protects from fire [3]. Various Experimental and numerical studies have been conducted under low cyclic reverse loading, which shows the composite section's good seismic behaviour (fairly enough deformation capacity and energy dissipation). At the same time, the seismic behaviour worsens for a higher axial load ratio[4–6]. Chen et al. [7] proposed the formula for the minimum transverse stirrup and embedded depth ratio forstirrup areas lessthanthe limiting value given by the Chinese code. The close-spaced tie bars are required to provide effective confinement, and a minimum shear strength should be maintained during inelastic deformation. They compared different codal computational methods against experimental results of axially compressed highstrength concrete composite columns and found that all codal provisions work adequately only over a small range of parameters. Among many design codes, Euro code 4 provides more accurate results as compared to others [3,8,9].

*Corresponding author. Tel: ++919675986781; E-mail address: ce20d027@smail.iitm.ac.in

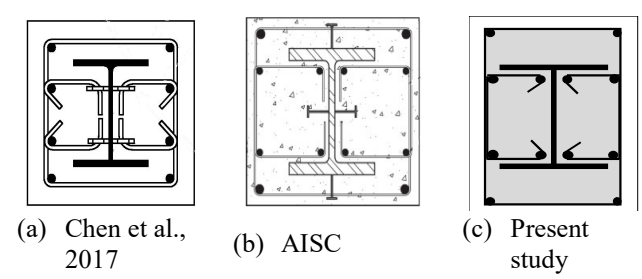


Fig. 1. Cross section of different encased columns

It is understood that the strength and deformation capacity can be increased by providing structural steel in the section.Based on Chen et al. [10] experimental results, structural steel reduces the transverse reinforcement criteria for high ductile members. The effect of special confining stirrups near structural steel on ductility is investigated in this study. As per codal provisions, the detailing of confining reinforcement is similar to the reinforced concrete column, but different confinement stirrup patterns areadopted for the encased composite column. A region of high concrete confinementnear web flanges junction increases the concrete crushing strain. While for less ductile members, the transverse reinforcement can be reduced for the composite columns. However, what degree of reduction can be provided to the composite column is not well understood and can be a part of future studies.AISC equation does not provide a reliable level of ductility performance, resultingin an unconservative according to the performance requirement for special moment frames [2]. AISC 341-16 suggested a special detailing of closed hoops and cross-ties, as shown in fig. 1(b); the steel shear connectors are provided for composite action between concrete and steel[10]. While Chen et al. [11] suggested tie connectors to connect the inner tie, as shown in fig. 1(a). Studs barely affected the performance of composite columns, as adequate bond exists between steel and concrete [6]. Welding tie connectors and shear connectors is a tedious job and not preferred by the industries. This study proposes a special detailing for moderate to highly ductile members without shear connectors and tie connectors, as shown in fig.1(c).

2. Confinement of concrete

Ductility is a significant criterion for measuring the inelastic behaviour of a member. For low seismic zones, moderately ductile members are required, and for high seismic zones, the required ductility can be achieved by special detailing of transverse reinforcement. The steel plasticity and confined concrete core provide more inelastic strain before failure. In the seismic design of the column, the potential plastic hinge regions need to be carefully detailed for ductility. As the steel section provides a large amount of plasticity, the ductility of the composite section primarily depends on the core confined concrete. The effective lateral confinement is generated by uniform hoop tension developed by transverse reinforcement. The effective confined core area is determined as a 2nd-degree polynomial (parabola) in the horizontal and vertical directions [12]. The horizontal legs are provided to increase the confined core area, and the spacing of the vertical stirrup governs the core concrete volume. The confined concrete is represented as shown in fig.2.

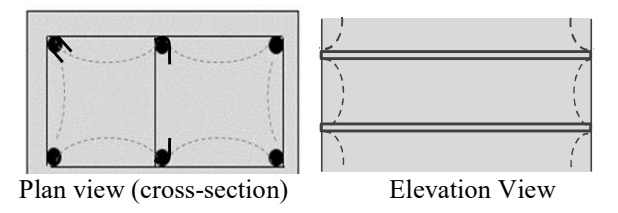


Fig. 2. Confinement of core concrete in RC sections

The ultimate compressive strain can be calculated based on the first hoop fracture. The buckling of the longitudinal bar is observed after the hoop fracture. Mander[12] proposed a rational method for longitudinal concrete compressive strain at first hoop fracture based on an energy balance approach. The most significant variable is the volumetric ratio of confining reinforcement (ρ_s).

Fire and corrosion are the major drawbacks of using only structural steel. The steel sharply loses its strength, stiffness and stability during the fire. Intumescent paints are available, which protect the fire but are costly and have drawbacks. Providing a concrete cover (fire concrete) for the steel section can be helpful in fire and prevent local buckling. The encased composite column may be as fireresistant as a reinforced concrete column. The thermal mass of concrete isolates the steel section, and the light reinforcement provides insulation during an earthquake. As per Indian standard, the minimum cover should be at least 40 mm for two-hour fire resistance. Here, 40mm unconfined concrete is provided as the cover, and a partially confined concrete is supplied with minimum reinforcement criteria, called fire concrete, as shown in fig. 3 (a). The partial confinement of fire concrete provides partial ductility and protects the steel flanges in the fire.

A large amount of rotation can be observed near the fixed end of a cantilever column subjected to lateral loading. The rotation at the plastic hinge provides rotational ductility without a significant increase in moment capacity. The plastic hinge length is spread over the column with an increasing axial load ratio. A high axial load adds an additional moment at the base hinge of the column, primarily known as the P- Δ effect. In this study,a WPB 250×250@67.21 kg/m section with flange slenderness(b/t) of 11.35 is selected, which comes under a semi-compact classification as per IS 800 (2007). An encased composite column is formed by encasing WPB 250×250at the centre of the RC section, as shown in fig. 3 (a). As the different parts of the section exhibit different confinement, the nominal cover for longitudinal reinforcement is assumed unconfined, and the fire concrete is partially confined concrete. The dashed line shows the highly confined concrete due to the flange and web of the section. The stress-strain curve for unconfined, partially confined, and highly confined is calculated based on Mander's rational formula. Figures 3(b) and (c) show that two types of probable splitting paths may appear for confined concrete. For a narrow steel section, concrete bursting may occur for a higher axial load ratio. Still, the chances of this type of probable cracking in WPB are less, as the highly confined concrete near the web flange junction prevents thisbursting. Fig. 3(c) investigates the chances of corner spalling of partially confined concrete. A cross tie near the flanges of the section,

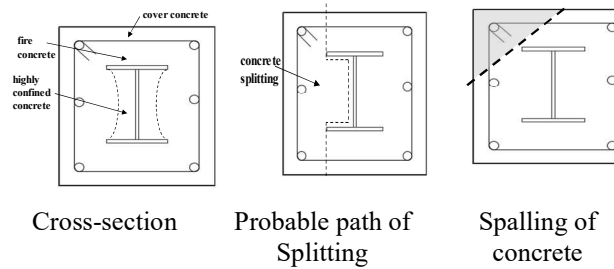
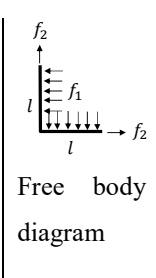


Fig. 3. Cross-section of the composite section with confinement and cracking path

The spalling force on the cross-section of the section is developed due to vertical pressure: $f_1 = \mu \sigma ls$ Where μ and s are the poison's ratio of the concrete and spacing of transverse reinforcement, respectively. The force resisted by transverse reinforcement is $f_2 = f_y A_t$. The relationship between clear length (l) and spacing (s) is calculated based on the criteria $(f_1 < f_2)$.



as shown in fig. 1(c) can delay partially confined concrete's crushing and provide better ductility. This study focused on how much an increase in displacement ductility, plastic hinge rotation and drift ratio could be achieved by providing a cross-tie. The concrete section is highly stressed due to the high load ratio and forces required by the transverse reinforcement to maintain the bursting pressure. Two types of confinement exist in the encased composite columns: (1) Stirrup induced confinement, which considers the stirrup volumetric ratio and spacing of transverse bar; (2) Structural steel induced confinement, which covers the high confinement zone as shown in fig. 3 (a).

The potential buckling mode and the corresponding buckling length of longitudinal bars depend on the geometrical and mechanical properties of both longitudinal and transverse reinforcement. Dhakal and Su (2018)[13] proposed a design recommendation to ensure the satisfactory buckling restraint of lateral ties. Lateral ties delay the buckling-induced instability until the desired level of ductility is achieved. The tie stiffness k_i is used to define the buckling of main bars between two consecutive ties derived from the energy-based approach.

3. FEM Modelling

3.1 Modelling approach

The parts of the encased composite column are modelled and assembled in finite element-based software (ABAQUS). Three types of effectively confined areasare considered for the encased column:unconfined, partially confined, and highly confined concrete, as shown in fig.3(a). Chen and Lin [1] defined confining factor for partial and highly confined concrete by varying the shape of structural steel and reinforcement layout. The high confinement can be simplified into rectangular sections up to half of the flange width [14].A 3D solid element (C3D8R, an 8-node linear brick with reduced integration) is available in the ABAQUS element library for concrete and steel sections, and a 2-node linear 3-D truss element (T3D2) for reinforcing bar and stirrups[15,16] is used. The concrete damage plasticity

(CDP) model is used for the plastic behaviour of concrete. Different mess size is tried for convergence issues and less computational time. A reasonable mess size of 20 mm for concrete and steel and 5 mm for reinforcing bars provides satisfactory results and less computational time.Fe345 grade of structural steel with an elastic modulus of 210 GPa and Poisson's ratio equal to 0.2 is provided in this analysis. The nonlinear part of the stress-strain curve is modelled as a plastic option available in ABAQUS.

3.2 Modelling of confined concrete

Based on Mander's rational equation, the stress-strain curves are plotted for confined and unconfined concrete and used for this analysis. Fig. 4 shows the uniaxial strain-stress curve for concrete in compression. The unconfined stress-strain curve for M30 grade of concrete is used in this study, in which ultimate strain (ε_{cu}) is taken as twice of ε_0 (ε_0 =0.002). The confined concrete compressive strength (f_{cc}) and ultimate confined strain (ε_{cu}) are used as proposed by Mander et al. [12]. The unconfined concrete is used for the typical confined section without a cross tie, while confined concrete is used in the core of the special confined section, as shown in fig.1 (c). The concrete near web-flange joints is highly confined and modelled separately. For a typical section without a cross tie, an unconfined stress-strain curve is used throughout the cross section as the concrete is partially confined.

The plastic behaviour of the concrete is modelled with a concrete damage parameter available in ABAQUS material library. The dilation angle $\phi=30^{0},$ flow potential eccentricity $\epsilon=0.1,~f_{b0}/f_{c0}\!=\!1.16,~K\!=0.667$ and viscosity parameter $\mu\!=0$ is used in this study [17]. The modelling of the special confined concrete is done separately and assembled with the model. The 'embedded region'interaction is used,in which the unconfined and confined concrete is assigned as a host region for embedded steel and reinforcement. The modelling of confined and unconfined concrete is shown in fig. 5.

1.1 Modelling of interface and initial geometric imperfection

The interaction of the steel, reinforcement and concrete parts is modelled using embedded elements available in ABAQUS library. The reinforcement and steel section is treated as an embedded region, while concrete behaves as a host region.

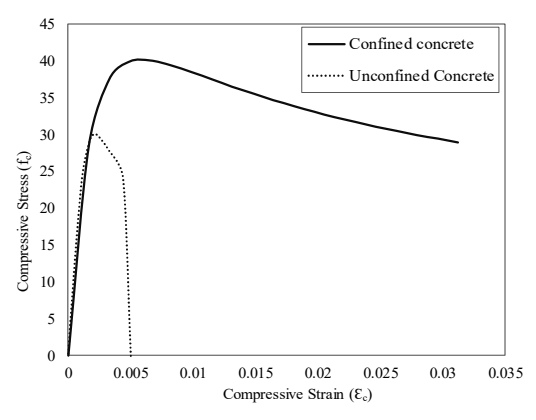


Fig.4. Stress-strain curve for confined and unconfined concrete in compression

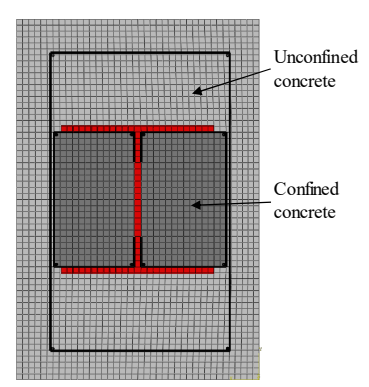


Fig. 5. FEM modelling of unconfined and confined encased steel concrete composite column

The buckling mode of the section is predicted with an eigenvalue analysis, and the eigenvalue is normalised to scale 1.0. The first Eigen mode is provided for the initial imperfection of encased composite column. The widely accepted initial geometric imperfection of L/2000 is considered, and based on this magnitude, a factored buckling mode is incorporated in the initial step of the model[15].

1.2 Boundary condition & load applications

The encased composite column is fixed at one end and free at the top. The fixity is obtained by restricting all the nodes for displacement and rotation. The loading is applied in two steps; in the first step,a defined axial load is applied on the top surface of the column as a pressure load and propagated in further analysis. In 2nd step of the loading, a lateral load is applied to the top of the cantilever-encased composite column. The total lateral forces at the fixed end are plotted with the applied displacement.

2. Validation of FEM modelling

In this study, the finite element model of an encased composite column is validated with the experimental result given by Lai et al. [9]. A concrete-encased column made with high-strength of concrete (C100) and structural steel (S355-H) is considered for the study. The inelastic stressstrain curve for high-strength concrete is required for FEM analysis. The post-peak branch of high-strength concrete is not captured in the experiment. The constitutive relation for concrete strength up to 100 MPa is given by Güleret al.[18], which is used here. A similar procedure in section3 is used for modelling the section. A 2800mm long specimen with a square cross-section (250mm×250mm) is selected. The steel area ratio and spacing of the transverse reinforcements are 10.02% and 100 mm, respectively. The horizontal and vertical displacement is plotted against axial load. Fig. 6shows the result obtained from the experiment and finite

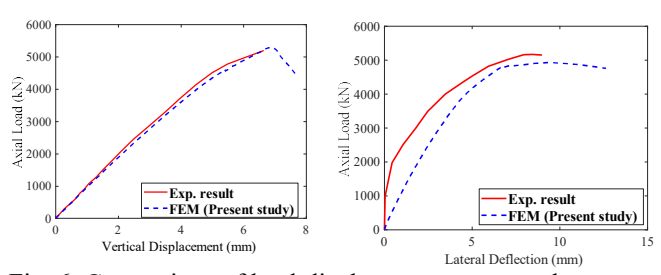


Fig. 6. Comparison of load-displacement response between

experimental and numerical analysis.

element model. The FEM results are reasonablymatching with experimental data. Due to the brittle nature of high-strength concrete, the post-peak deflection is not clearly captured in the experiment.

3. Results

3.1 Failure mode

The typical failure sequencing for the composite column is yielding of tensile reinforcement, crushing ofconcrete and buckling of longitudinal reinforcement. For encased sections, crushingof fire concrete reduces partial ductility. However, the highly confined concrete gives adequate ductility to the section. The local buckling of steel flanges is resisted by concrete near to flange and provides a larger ductility capacity. The failure of the composite section is definedat the reduction of the maximum strength by 15%, as shown in fig. 9.Fig. 7 shows the actual and idealised momentcurvature curves for the section; after the reduction of moment capacity by 15%, the encased section continues to take significant moments for higher curvatures. The idealised moment-curvature of reinforced concrete, encased section, and structural steel is plotted as shown in fig. 7. The crushing of partially confined concrete itself reduces the moment capacity by more than 15%. Based on the idealised bilinear moment-curvature curve, the encased section's ductility is less than the RC section for the zero axial load ratio. Whereas for higher axial loads, the situation gets reversed, as explained in section 7.1. After spalling of partially confined concrete, the core of the composite section (highly confined concrete and structural steel) continues to take a moment up to a significant curvature. As concrete is brittle, the special detailing of transverse reinforcement provides large curvature ductility. The confined concrete exhibits significant rotation and hence provides large curvature before failure.

The bulging of concrete near the fixed end (front-left in Fig. 8) is obtained for the high axial load ratio. The stress contour of the longitudinal and transverse bar on the compression side shows the failure of the reinforcing bar. The failure of transverse reinforcement can cause the buckling of compression reinforcement. Fig. 8 shows the deformed shape, stress contour and plasticity spread.

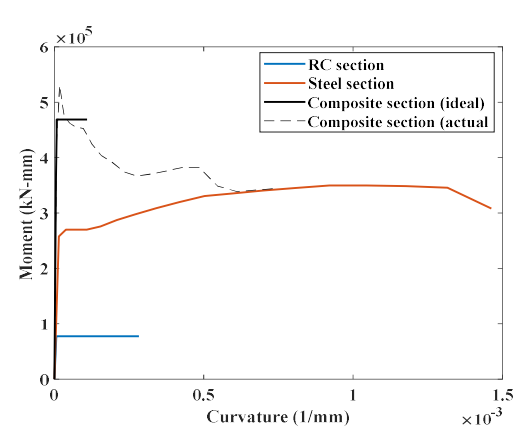


Fig. 7. Moment curvature of the sections at zero axial load

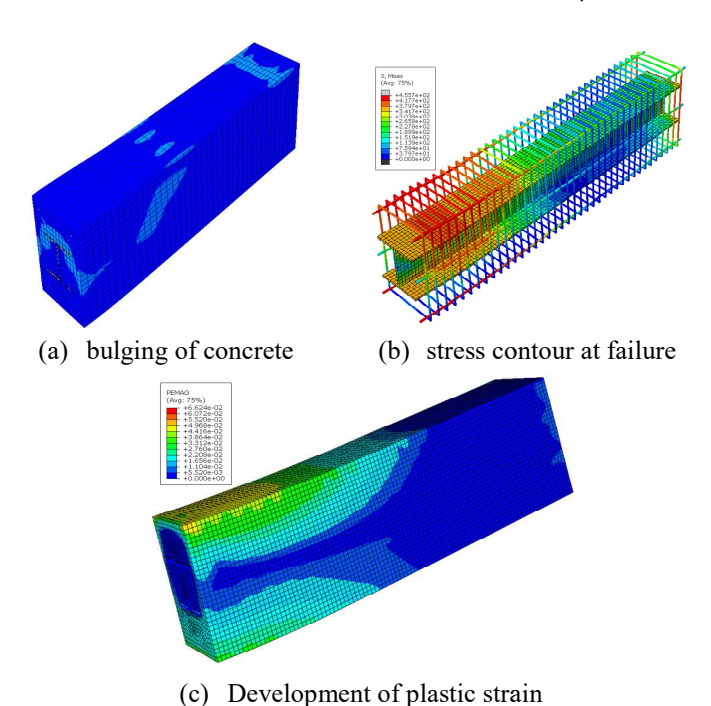


Fig. 8. Failure mode and stress distribution of the model

3.2 Deformation capacity

The inelastic deformation capacity is measured with the member's displacement ductility, plastic hinge rotation and drift ratio capacity. The displacement ductility factor (μ_{Δ}) is the primary representation of the deformation capacity of the member. The displacement ductility factor is defined as the ratio of ultimate displacement (Δ_u) to yield displacement (Δ_y) .

$$\mu_{\Delta} = \frac{\Delta_u}{\Delta_v}$$

The ultimate displacement corresponds to the residual lateral force carrying capacity that has declined to $0.85H_{max}$; the yield displacement is defined as the displacement corresponding to the secant slope at $0.75~H_{max}$, as shown in fig.9.

The plastic hinge rotation (θ_p) is defined as the ratio of difference of ultimate and yield displacement to the length of the member.

$$\theta_p = \frac{\Delta_{u-\Delta_y}}{l}.$$

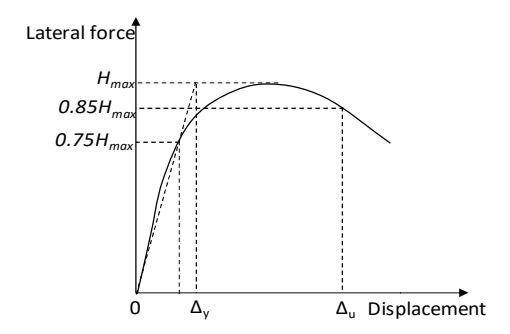


Fig. 9. Definition of yield and ultimate displacement

The member's lateral drift ratio capacity (α_u) is defined as the ratio of ultimate deformation to the effective column length. Further sections explain each case's displacement ductility factor, plastic hinge rotation, and drift ratio.

4. Ductility based on special detailing

As mentioned earlier, the increase in the area of transverse reinforcement and reduction in spacing provides more confinement to the column. The primary concern of the composite column is the detailing of transverse bar; a large ductility can be achieved by providing special detailing of transverse bars at close spacing. Fig. 3(a) showsthat the effective confinement area can exhibit large ductility while the column failure is due to the crushing of partially confined concrete. In this study, the effect of special detailing is investigated. The effective confined area can be increased by providing an additional cross-tie bar, as shown in fig 1(c). For highly ductile members, AISC provides a complex detailing of transverse reinforcement with shear connectors to prevent the slippage of concrete on steel flanges. As per the Indian code for composite construction, IS 11384, the shear transfer between concrete and steel is ensured through bonds up to shear stresses of 0.3 N/mm²;mechanical shear connectors should be provided beyond these stresses. The shear connectors complicate the section, and welding the shear connector is a tedious job. A similar section provided by AISC is used without steel anchors in this study and compared with the typical encased composite column. The effective fully confining stress is achieved by giving the cross-tie. The confinement detailing of the special detailed encased composite section is shown in fig.10.

The stress-strain curve for unconfined and confined concrete was explained in modelling section 3.2. The post-peak strength reduction is remarkably less after providing a cross tie, as shown in fig.11. The displacement ductility, plastic hinge rotations and drift ratios for a regular and special detailed column are summarised in Table 1.

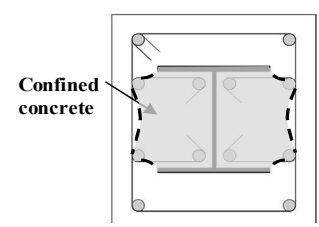


Fig. 10. Effectively confined core for encased composite column

Table 1. Effect of special confinement

	ρ_{axial}	μ_{Δ}	θ_p	α_{u}
Regular confinement	0	3.53	0.034	4.7
	0.2	3.11	0.025	3.7
	0.4	3.08	0.021	3.1
	0.6	2.94	0.018	2.7
	0.8	2.88	0.016	2.4
	0	>8.2	-	>7.5
Special confinement	0.2	>8.2	-	>7.5
	0.4	8.15	0.066	7.5
	0.6	5.77	0.043	5.2
	0.8	4.70	0.032	4.0

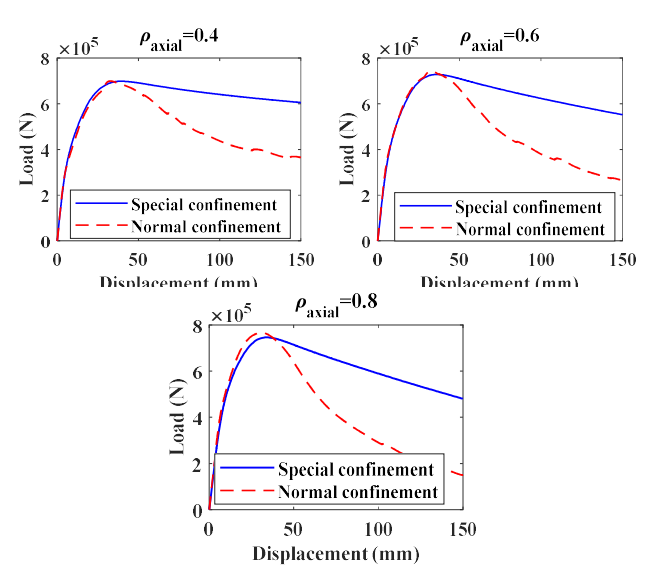


Fig. 11. Load displacement response for regular and special confined concrete

The special confined section provides a displacement ductility ratio of more than 8.2 compared to 3.53 for the typical section. For a higher axial load ratio (ρ_{axial} =0.8) also, the ductility ratio is quite reasonable (>4) for a special confined section.

For the higher axial load ratio (0.8), 100% and 67% increments are observed for plastic hinge rotation and drift ratio, respectively, which are pretty high. The results confirm that a good amount of ductility can be achieved by special detailing of transverse reinforcement.

5. Parametric study

5.1 Effect of axial load ratio

The ratio of applied axial load to the column's designed axial load carrying capacity is defined asthe axial load ratio (ρ_{axial}). The designed axial load carrying capacity of the column (P_d) at the ultimate stage is given by IS 11384-2019 as: $P_d = \frac{A_s f_y}{\gamma_{mo}} + \frac{A_s t f_{yk}}{\gamma_k} + \frac{0.68}{\gamma_c}$

Where γ_{m0} , γ_k and γ_c are partial safety factors for concrete, structural steel and reinforcement, respectively[19].

Five different axial load ratios ranging from 0 to 0.8 are considered in this study. The post-peak deflection gradually increases with the axial load ratio. When an axial load is applied to a column, it induces two effects: one is the compressive membrane effect that reduces the lateral column deflection, and the other one is the P- Δ effect that amplifies the lateral column deflection. When the axial load ratio is small, the compressive membrane effect is more dominant and vice versa[20]. The steel section is known to be ductile and provides more ductility to the composite section. A semi-compact WPB 250×250@67.21kg/m section is encased in the concrete preventing the local buckling of the flange. First, the lateral load-deformation capacity was calculated for the pure steel section (WPB 250×250). For a high axial load ratio, the compression flange starts locallybuckling, and the column shows less ductility, as shown in fig. 12. The second-order effect is high for high ρ_{axial} and a small horizontal deflection

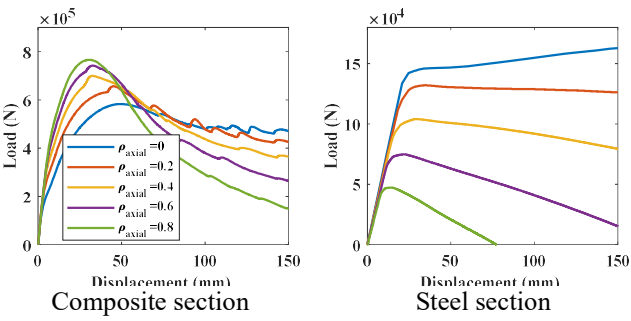


Fig. 12. Load displacement response for different axial load

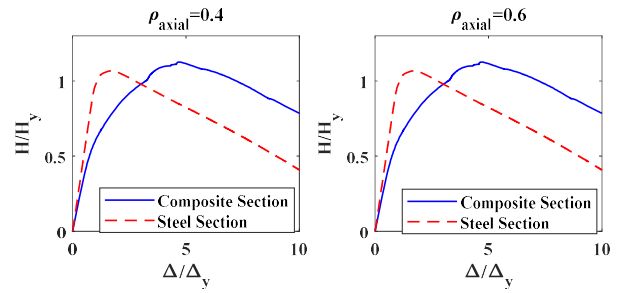


Fig. 13. Load displacement response for steel and encased section

(Δ) amplifies the column's bending (P- Δ) effect significantly. As in figure 12, the steel member's lateral load capacity and inelastic deflection are much less for higher ρ_{axial} .

On the contrary, the composite section does not show the column's sharp reduction of load capacity for a high axial load ratio. The composite section is analysed for different axial load ratios, and its load-deformation response is shown in fig. 12,which shows good deformation capacity for encased composite sections for higher axial load ratios. The bulging of concrete near the fixed end is observed for a high axial load ratio, gradually reducing the strength. The increase in the displacement ductility for the composite section is primarily due to the reduction of yield displacement as the stiffness of the section increases. The yield displacement and failure displacement are calculated as defined in section 5.2. The normalised horizontal force (H/H_y) is plotted against normalised displacement (Δ/Δ_y) for two different axial load ratios, as shown in fig. 13.

5.2 Effect of steel contribution ratio

The steel contribution ratio is an important design parameter for composite sections. The interaction diagram of the composite column is highly influenced by the steel contribution ratio [21]. As per IS 11384 (2019), the steel contribution (δ) is defined as $\delta = \frac{A_s f_y}{P_d Y_m}$. The six encased structural steel sections are selected for parametric study. The web and flange slenderness of the sections are calculated and classed as semi-compact and compact as per IS 800-2007[22]. The displacement ductility, plastic hinge rotation and drift ratio for different sections are calculated and summarised in table 2. Due to space constraints, the lateral load-displacement curve for the six sections is plotted for $\rho_{\text{axial}} = 0.4$ only.

Table 2. Ductility for different steel contribution ratios

Dimensions	Structural steel	δ	μ_{Δ}	θ_p	$\alpha_{\rm u}$
COM 400×600	WPB 220×40.40	0.43	3.68	0.024	3.2
COM 400×600	WPB 240×47.39	0.48	3.63	0.023	3.2
COM 400×600	WPB 200 \times 50.92	0.50	3.11	0.02	3.0
COM 400×600	WPB 240 \times 60.32	0.55	3.14	0.02	3.0
COM 400×600	WPB 250×67.21	0.58	3.08	0.021	3.1
COM 400×600	NPB 350×250×79.1	0.64	3.59	0.025	3.4

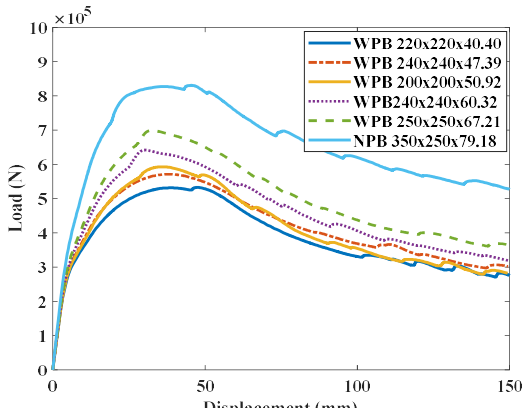


Fig. 14. Load displacement response for different steel contributions at ρ_{axia} =0.4

The result shows the expected behaviour that by providing a higher steel contribution ratio, the stiffness and strength of the composite column increase, as shown in fig. 14.

By increasing the steel contribution ratio from 0.43 to 0.64, the displacement ductility, plastic hinge rotations and drift ratios arenot changing much. Table 2 shows that the displacement ductility decreases with increasing steel contribution ratio except for NPB 350×250×79.1. As stiffness and strength increase, drift ratio and plastic hinge rotation do not vary much by changing the steel contribution ratio. Section 7.3 shows that the steel section flange width to section depth ratio comes across as the more significant governing criteria for ductile designing rather than the steel contribution ratio.

5.3 Effect of section width to depth ratio

The effect of structural steel width to depth ratio is investigated in this study. Two structural steel WPB 250×67.21 and NPB 350×250×79.1 sections with width to depth ratios of 1.02 and 0.73 are used to form the regular and deep encased sections, respectively. IS 11384 does not specify the limiting flange slenderness of the steel for the composite column. The flange slenderness of regular and deep steel sections is 11.35 and 8.93, respectively, satisfying the criteria for semi-compact and compact sections. The displacement ductility, plastic hinge rotations and drift ratios are calculated for different axial load ratios and summarisedin table 3. The sections are designated as S-20 and SD-20, where Srepresents the regular composite column (WPB

Table 3. Effect of member width to depth ratio

Steel section	μ_{Δ}	θ_p	$\alpha_{\rm u}$	
S-00	3.53	0.034	4.7	
S-20	3.11	0.025	3.7	
S-40	3.08	0.021	3.1	
S-60	2.94	0.018	2.7	
S-80	2.88	0.016	2.4	
SD-00	6.56	0.064	7.5	
SD-20	4.76	0.037	4.7	
SD-40	3.86	0.025	3.4	
SD-60	3.57	0.021	3.0	
SD-80	3.02	0.017	2.5	

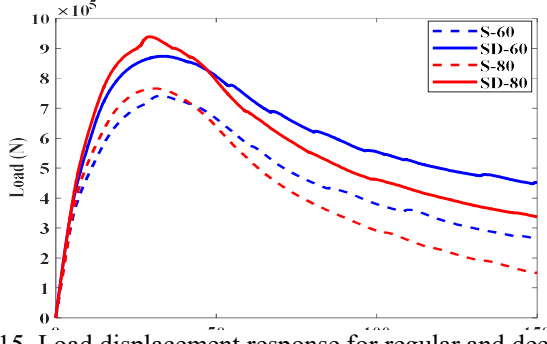


Fig. 15. Load displacement response for regular and deep section

250×250×67.21), SD represents the deep section (NPB 350×250×79.1), and the later part of the ID represents the percentage of axial load ratio on the column.

Fig. 15 shows a significant increase in displacement ductility for deep sections. The changes are more prominent for the lower axial load ratio, whilemore than three displacement ductility is observed for the deep section at higher axial load ratios. The increment of plastic hinge rotation and drift ratio is up to 88% and 59% for regular and deep sections, respectively. In comparison, the steel contribution ratio for NPB 350×250×79.1 is only 10.3% higher than WPB 250×250×67.21.

5.4 Effect of transverse reinforcement spacing

The stirrup ratio increases the ductility by increasing the core confined concrete area [7]. Closely spaced tie bars increase the core confined area, resulting ina higher strain capacity of the concrete. The effect of transverse reinforcement is evaluated for different axial load ratios. This study evaluates an encased column with 100 mm and 50 mm tie bar spacing. The displacement ductility, plastic hinge rotations and drift ratios are investigated for different axial load ratios and summarised in table 4.

As shown in Table 4, the displacement ductility, plastic hinge rotations and drift ratios increaseby 42%, 56% and 43% for zero axial load ratio, respectively. The 50 mm spaced specimen shows a displacement ductility ratio of more than three, even for a higher axial load ratio. For an axial load ratio of more than 0.2, the plastic hinge rotation barely shows an increase of less than 20%. The lateral load-displacement curve for a higher axial load ratio (0.6 and 0.8) is plotted in Fig. 16.

Table 4. Effect of transverse reinforcement

Tie spacing	ρ _{axial}	∆ _y	∆ _u	μ_{Δ}	θ_p	α _u (%)
100 mm	0	26.7	94.0	3.53	0.034	4.7
	0.2	23.7	73.8	3.11	0.025	3.7
	0.4	19.9	61.2	3.08	0.021	3.1
	0.6	18.4	54.1	2.94	0.018	2.7
	0.8	16.9	48.8	2.88	0.016	2.4
50 mm	0	26.7	133	4.99	0.053	6.7
	0.2	23.7	81.4	3.43	0.029	4.1
	0.4	19.9	69.9	3.52	0.025	3.5
	0.6	18.4	60.2	3.27	0.021	3.0
	0.8	16.9	54.1	3.19	0.019	2.7

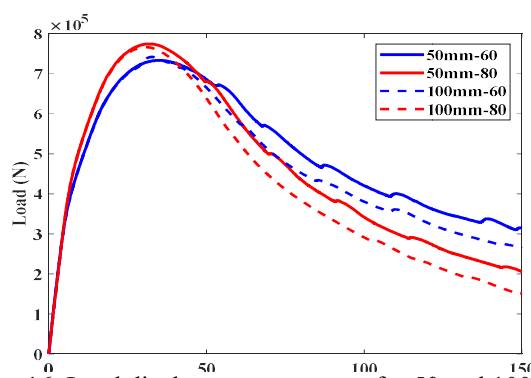


Fig. 16. Load displacement response for 50 and 100 mm spacing of tie bar

6. Conclusions

This study uses a nonlinear 3D modelling of encased concrete composite columns. Concrete confinement is investigated by providing special detailing of the transverse reinforcement. The displacement ductility factor, plastic hinge rotation and drift ratio are evaluated for different axial load ratios. The parametric study has been carried out by varying the axial load ratio, steel contribution ratio, steel width to depth ratio and transverse reinforcement spacing. This study finds the following outcomes for an encased composite column.

- 1. The special detailing of transverse reinforcement enhances the ductility factors significantly. The regular detailed encased composite column does not show good ductile behaviour for a higher axial load ratio. Even for a high axial load ratio (ρ_{axial} >0.6), the displacement ductility comes out to be>4, indicating the good deformability of the special encased section.
- The deformation capacity is not too sensitive tothe steel contribution ratio, although the stiffness and strength capacity increase.
- 3. The steel width-to-depth ratio is a more governing parameter for the seismic design of composite columns. A higher width-to-depth ratio increases deformation capacity up to 88% by confining more concrete area.
- 4. The effect of spacing of transverse reinforcement is investigated; about a 42% increment in displacement ductility is observed for a 50 mm spaced stirrup section over a 100 mm spaced

section. Providing stirrups too close is practically difficult and creates concrete pouring congestion. Here a spacing of 50 mm of transverse reinforcement shows good ductility at an axial load ratio of 0.6.

Disclosures

Free Access to this article is sponsored by SARL ALPHA CRISTO INDUSTRIAL.

References

- [1] Chen CC, Lin NJ. Analytical model for predicting axial capacity and behavior of concrete encased steel composite stub columns. J Constr Steel Res 2006;62:424–33. doi:10.1016/j.jcsr.2005.04.021.
- [2] Chen CC, Chen CC, Hoang TT. Role of concrete confinement of wideflange structural steel shape in steel reinforced concrete columns under cyclic loading. Eng Struct 2016;110:79–87. doi:10.1016/j.engstruct.2015.12.002.
- [3] Mirza SA, Lacroix EA. Comparative Strength Analyses of Concrete-Encased Steel Composite Columns. J Struct Eng 2004;130:1941–53. doi:10.1061/(asce)0733-9445(2004)130:12(1941).
- [4] Campian C, Nagy Z, Pop M. Behavior of fully encased steel-concrete composite columns subjected to monotonic and cyclic loading. Procedia Eng 2015;117:439–51. doi:10.1016/j.proeng.2015.08.193.
- [5] Gautham A, Sahoo DR. Behavior of steel-reinforced composite concrete columns under combined axial and lateral cyclic loading. J Build Eng 2021;39:102305. doi:10.1016/j.jobe.2021.102305.
- [6] Zhu W, Jia J, Gao J, Zhang F. Experimental study on steel reinforced high-strength concrete columns under cyclic lateral force and constant axial load. Eng Struct 2016;125:191–204. doi:10.1016/j.engstruct.2016.07.018.
- [7] Chen C, Wang C, Sun H. Experimental Study on Seismic Behavior of Full Encased Steel-Concrete Composite Columns. J Struct Eng 2014;140:04014024. doi:10.1061/(asce)st.1943-541x.0000951.
- [8] Venkateshwaran A, Lai BL, Liew JYR. Buckling resistance of steel fibre-reinforced concrete encased steel composite columns. J Constr Steel Res 2022;190:107140. doi:10.1016/j.jcsr.2022.107140.
- [9] Lai B, Richard Liew JY, Wang T. Buckling behaviour of high strength concrete encased steel composite columns. J Constr Steel Res 2019;154:27–42. doi:10.1016/j.jcsr.2018.11.023.
- [10] AISC 360-16. Specification for Structural Steel Buildings, an American National Standard. Am Inst Steel Constr Chicago 2016:612.
- [11] Chen CC, Chen CC, Shen JH. Effects of steel-to-member depth ratio and axial load on flexural ductility of concrete-encased steel composite columns. Eng Struct 2018;155:157–66. doi:10.1016/j.engstruct.2017.11.036.
- [12] Mander JB. MJNP, Park R. THEORETICAL STRESS-STRAIN MODEL FOR CONFINED CONCRETE. J Struct Eng 1989;114:1804–26.
- [13] Dhakal RP, Su J. Design of transverse reinforcement to avoid premature buckling of main bars. Earthq Eng Struct Dyn 2018;47:147– 68. doi:10.1002/eqe.2944.
- [14] Mirza SA, Skrabek BW. Statistical Analysis of Slender Composite Beam-Column Strength. J Struct Eng 1992;118:1312–32. doi:10.1061/(asce)0733-9445(1992)118:5(1312).
- [15] Ellobody E, Young B. Numerical simulation of concrete encased steel composite columns. J Constr Steel Res 2011;67:211–22.

- doi:10.1016/j.jcsr.2010.08.003.
- [16] Ellobody E, Young B, Lam D. Eccentrically loaded concrete encased steel composite columns. Thin-Walled Struct 2011;49:53–65. doi:10.1016/j.tws.2010.08.006.
- [17] Han LH, Yao GH, Tao Z. Performance of concrete-filled thin-walled steel tubes under pure torsion. Thin-Walled Struct 2007;45:24–36. doi:10.1016/j.tws.2007.01.008.
- [18] Güler K, Demir F, Pakdamar F. Stress-strain modelling of high strength concrete by fuzzy logic approach. Constr Build Mater 2012;37:680–4. doi:10.1016/j.conbuildmat.2012.07.069.
- [19] IS:11384. Composite construction in structural steel and concrete Code of practice 2019;38.
- [20] Zhao GT, Zhang MX, Li YH. Behavior of slender steel concrete composite columns in eccentric loading. J Shanghai Univ 2009;13:481–8. doi:10.1007/s11741-009-0611-2.
- [21] Rosmanit M, Pařenica P. Capacity of composite steel-concrete columns. Procedia Eng 2013;65:428–33. doi:10.1016/j.proeng.2013.09.067.
- [22] IS:800-2007. IS: 800 2007, Indian standard code of practice for general construction in steel. Bur Indian Stand New Delhi 2007.